SPATIAL SPARSITY AWARE EXPLAINABLE DEEP LEARNING-BASED LANDSLIDE SUSCEPTIBILITY MAPPING: APPLICATION TO A HILL DISTRICT, BANGLADESH

Author's Name:

Golam Murad[1], Md. Aftabur Rahman[2*], Hideaki Yasuhara[3]

Authors Affiliation:

[1]Graduate, Department of Civil Engineering, Chittagong University of Engineering & Technology, Chattogram-4349, Bangladesh, Email: u1901087@student.cuet.ac.bd

[2]Professor, Department of Civil Engineering, Chittagong University of Engineering & Technology, Chattogram-4349, Bangladesh, Email: maftabur@cuet.ac.bd

[3]Professor, Department of Urban Management, Kyoto University, Kyoto, Japan, Email: yasuhara.hideaki.7p@kyoto-u.ac.jp

*Corresponding Author: Md. Aftabur Rahman, Email: maftabur@cuet.ac.bd

SPATIAL SPARSITY AWARE EXPLAINABLE DEEP LEARNING-BASED LANDSLIDE SUSCEPTIBILITY MAPPING: APPLICATION TO A HILL DISTRICT, BANGLADESH

ABSTRACT

Landslide susceptibility mapping is a critical disaster risk management tool in mountainous regions, particularly in developing countries and in regions where development is ongoing or planned. This research introduces a novel approach to landslide susceptibility mapping that addresses the persistent challenge of spatial sparsity in landslide datasets, particularly in developing countries where strong monitoring of hill slopes is seldom available. A methodological framework that addresses data sparsity and explainable artificial intelligence (XAI) has been developed to enhance the accuracy of landslide susceptibility mapping, particularly in datasets that are limited or sparsely distributed. A landslide susceptibility map for Rangamati, the largest district of Bangladesh and part of the rugged, hilly Chittagong Hill Tract Region along the Bangladesh-India border, has been prepared using an updated methodological framework. The methodological framework first quantifies spatial sparsity through Voronoi-based clustering and spatial autocorrelation metrics (Getis-Ord Gi* and Moran's I), then implements sparsity mitigation techniques using DBSCAN clustering and Spatial density analysis. The research has examined twelve landslide conditioning factors derived from remote sensing data, including topographic, hydrological, and environmental variables. Three deep learning architectures—Deep Neural Network (DNN), one-dimensional Convolutional Neural Network (1D-CNN), and Long Short-Term Memory (LSTM)—have been implemented on both the original and sparsity-mitigated datasets. Comparative analysis revealed that the 1D-CNN model applied to the sparsity-free dataset achieved superior performance with an AUC of 0.9625, accuracy of 0.89, precision of 0.914, and F1-score of 0.853. SHAP analysis has provided unprecedented insights into feature importance, demonstrating that spatial context features. Despite limited data and computational constraints, this represents a significant improvement over models trained on the original dataset. The study demonstrates that addressing spatial sparsity before implementing deep learning algorithms substantially enhances landslide susceptibility mapping accuracy, providing a more reliable foundation for disaster risk reduction strategies. The framework demonstrates that addressing spatial sparsity before applying deep learning algorithms substantially improves prediction reliability, while XAI techniques ensure model transparency, which is essential for stakeholder confidence and operational implementation in disaster risk management scenarios.

Keywords: Landslide Susceptibility, Rangamati, Deep Learning, Spatial Sparsity, DBSCAN, Moran I, Getis-Ord Gi*, DNN, CNN, LSTM.

INTRODUCTION

Landslides are one of the world's most dangerous and destructive natural hazards, resulting in thousands of lives and substantial damage to the built environment and infrastructure. The global infrastructure and economic losses from landslides and landslide-induced flows are significant, as substantiated by studies worldwide(Song et al., 2024). With rapid urbanization, demand for space is high, especially in densely populated areas; as a result, development in mountainous or hilly regions is expanding globally. Besides that, the detached soil mass may travel at very high velocity and reach the distal end, eventually damaging everything along its flow path, as evidenced historically and even in recent years(Rahman & Konagai, 2017, 2018). The clever approach is to understand the susceptibility of hilly terrain; at the very first stage, identifying risky areas through a regional-scale hazard map is of primary interest to academics and professionals. To date, many studies have been conducted to develop landslide susceptibility maps, considering various factors. Advances in computational facilities enable researchers and professionals to use sophisticated machine learning (ML) algorithms for hazard quantification. Extensive research has focused on landslide susceptibility assessment using ML approaches, while the sparsity of the inventory dataset is a crucial factor for prediction and estimation accuracy. Spatial sparsity arises from the highly heterogeneous nature of the data points and poses a grand challenge, as it can introduce an inherent bias in model predictions (Yi et al., 2020). To make it clear, the landslide inventory is one of the most important input parameters that significantly influence the hazard response, and unfortunately, inventory data are not available for all locations due to a lack of monitoring facilities and limited awareness, especially in developing or least-developed countries. This spatial sparsity may weaken the performance of the model, leading to unreliable susceptibility maps. Classically developed methods, such as spatial interpolation and data aggregation, are often not adequately applied to the complex spatial relationships among landslide conditioning factors (Dahim et al., 2023).

The recent progress in deep learning architectures, Deep Neural Networks (DNN), Convolutional Neural Networks(CNN), Recurrent Neural Networks(RNN), Long Short-Term Memory (LSTM), and hybrid models (Azarafza et al., 2021) gained attraction that enables the extraction of complex topological features (M. A. Hussain et al., 2023b). Specifically, LSTM can capture temporal dependencies between landslide conditioning factors (e.g., rainfall patterns and vegetation change) and has often been shown to outperform conventional statistical and machine-learning models (LeCun et al., 2015a). Developments in spatial clustering in the last few years have recently piquing interest in solving the problem of spatial sparsity. For example, the Density-Based Spatial Clustering of Applications with the Noise (Schubert et al., 2017)algorithm has shown practical cluster detection ability in data of different densities, assists in the identification of high-density clusters and points in very low-density noise regions (Shen et al., 2016), and in the end helps improve data sparsity. However, there is a significant research gap in integrating spatial sparsity mitigation techniques with deep learning models, especially for landslide hazard estimation. Data availability is scarce, resources are limited, and rugged terrain complicates data collection (Hafsa et al., 2022). In a nutshell, the limited data pose remarkable challenges for obtaining quantitative values and shed light on data scarcity. Keeping the issue in the spotlight, this research aims to develop a comprehensive and integrated approach to prepare a

landslide susceptibility map, addressing the lack of influencing parameters; to be specific, the limited inventory data, which is mostly constrained by the constraints in hazard mapping, has been discussed in estimating landslide susceptibility mapping.

This study employs spatial sparsity(Hawkins, 1980) detection and quantification techniques to assess landslide conditioning datasets. Approaches such as Voronoi-based clustering (Okabe et al., 2000),(Miao et al., 2016), and spatial autocorrelation metrics, including Getis-Ord Gi*(Getis & Ord, 1992a) and Moran's I(Anselin, 1995), are utilized to examine spatial sparsity patterns. Density-Based Spatial Clustering of Applications with Noise (DBSCAN)(Ester et al., 1996a), (Han et al., 2023), and spatial density analysis(*Density Estimation for Statistics and Data Analysis | Bernard. W. Silv*, n.d.),(Parzen, 1962) are applied to mitigate the effects of sparsity, enhancing the dataset with clustering and density-related features. Three deep learning models—DNN, 1D CNN, and LSTM—were applied to the original and improved datasets. Then, a meaningful high-resolution landslide susceptibility map was produced to aid disaster risk management and urban planning(LeCun et al., 2015).The research methodology follows a structured multi-step approach, beginning with assessing spatial sparsity using Voronoi-based clustering and spatial autocorrelation analyses(Yang et al., 2018). After specifying the spatial sparsity of the data set, DBSCAN clustering and spatial density were used to enhance the data set with additional spatial clustering features. Finally, the viability of achieving spatial sparsity is quantified by comparing models trained on the original and enhanced datasets and by evaluating statistical metrics of model performance (Bradley, 1997a). As a case study, the Rangamati district, the largest hill district and rich in geological and geomorphological features, was selected to address the spatial sparsity of the landslide inventory and to produce a more precise landslide susceptibility map. The following sections discuss in detail the methodology and results of this research work.

DETERMINATION OF SPATIAL SPARSITY AND MITIGATION

The research methodology followed a systematic approach designed to address spatial sparsity and implement deep learning models for landslide susceptibility mapping. The first phase involved quantifying spatial sparsity in the landslide inventory using three complementary techniques: Voronoi-Based Clustering, Getis-Ord Gi*, and Moran's I.

Spatial Sparsity: Voronoi-Based Clustering

Voronoi-based clustering is a sophisticated spatial analysis that combines two popular methods: Voronoi diagrams and proximity relationships. It forms intuitive spatial boundaries such that each region contains all points closer to a particular seed point than any other. Each region (or Voronoi cell) contains all points closest to a given centre.(Okabe et al., 2000). Formally, the Voronoi cell of a point in a set X is shown as follows:

$$VorX(y) \coloneqq u \in R^n : y \in argmin_{(x \in X)} \parallel x - u \parallel 2 \qquad (1)$$

This clustering approach is efficient for spatial data, offering a natural way to visualize how points relate based on distance(Boonprong et al., 2024). Its principal benefit is the visual representation of relationships in space, with clear cluster boundaries that make patterns evident to analysts and stakeholders alike. However,

Voronoi-based clustering is susceptible to clusters being forced into the same hyperplane, leading to instability in the inherent Voronoi tessellation of the data samples. To mitigate such clustering tendencies, according to (Byers & Raftery, 1998), An addition of small random noise N ($0,10^{-6}$) to the data points was considered to improve the robustness of the clustering process. This slight shift disrupts the perfect positions without significantly altering the data, resulting in more robust, better-centered Voronoi cells. A polygon encloses each landslide point to represent its potential influence in space (Guzzetti et al., 2012a). The large Voronoi cell exists as spatial sparsity in areas with sparse landslide occurrences. High-density regions highlight clustered patterns with more miniature, dense lops in high-occurrence areas (Yang et al., 2021). These results offer clear visual proof of spatial sparsity in this respect and further indicate that Voronoi-based clustering is a powerful method for characterizing landslide spatial distribution (Andronov et al., 2016).

Spatial Autocorrelation Metrics: Getis-Ord Gi* & Moran's I

The Getis-Ord Gi* statistic is a local spatial autocorrelation statistic that detects statistically significant hotspots (clusters of high values) and cold spots (clusters of low values) within a study area(Getis & Ord, 1992b). It can identify hotspots or cold spots where high or low values of a variable are clustered more closely than expected by chance. Precisely, the Getis-Ord Gi*(Ord & Getis, 1995)The statistic was calculated to capture local spatial clustering patterns. The landslide data was formatted as a GeoDataFrame, and then a binary, row-standardized spatial weights matrix (Griffith, 2021) was generated using a distance band threshold of 0.05 degrees (~5.5 km). This threshold enabled the capture of meaningful neighborhood effects without excessive smoothing that would obscure local structure. This indicates that only truly proximate landslide locations affected one another's statistical values. The 0.05-degree threshold, corresponding to about 5.5 km at mid-latitudes, aligned with the geomorphological processes governing landslide occurrences(Guzzetti et al., 2012b). In this case, Gi* Z-scores were projected using a cool warm colour map, where more extensive (i.e., more positive) Z-scores imply local clustering. This allowed for accounting for neighborhood influences across variations in density and robustly highlighted localized patterns and outliers in the distribution of landslides(Haining, 2003).

Moran's I is one of the most widely used statistical tools that simultaneously measures spatial autocorrelation based on feature locations and values(Isnan et al., 2025). Given a set of features and an associated attribute, it evaluates whether the pattern expressed is clustered, dispersed, or random(Memisoglu Baykal, 2025a). In this research, Moran's I was used to assess global spatial autocorrelation, as introduced by Patrick Alfred Pierce Moran. Spatial autocorrelation is multidimensional and multivariate, unlike one-dimensional autocorrelation, making its analysis more complex(Chen, 2023). Moran's I test statistic is fundamentally a well-normalized quadratic form of the tested variables, so this is an extremely popular test for inspecting spatial dependence(Memisoglu Baykal, 2025b). Moran's I was calculated by comparing the value of each feature to its neighbor's, determined by a spatial weight matrix. The formula is:

$$I = \frac{n}{W} \frac{\sum_{i=1}^{n} \sum_{j=1}^{n} w_{ij}(x_i - \bar{x})(x_j - \bar{x})}{\sum_{i=1}^{n}(x_i - \bar{x})^2} \quad (2)$$

where n is the number of spatial units, w_{ij} is the weight between units i and j, x_i and x_j are the values, $\bar{x}$ is the mean, and W is the sum of weights. The Positive cross-products (both values above or below the mean) suggest clustering. On the other hand, negative ones indicate dispersion. Moran's I was computed using the k-Nearest Neighbors (k=5) (Bivand et al., 2013) weights matrix to assess global spatial autocorrelation in this study. The positive autocorrelation indicates the uneven spatial distribution of landslide data(Malamud et al., 2004), further justifying the need for sparsity mitigation techniques.

Sparsity Mitigation Techniques: DBSCAN Clustering for Sparse Regions

DBSCAN - Density-Based Spatial Clustering of Applications with Noise finds core samples of high density and expands clusters from them. It is Suitable for data that contains clusters of similar density(Ester et al., 1996b) and it has a worst-case memory complexity of $O(n^2)$, which can occur when the eps parameter is significant, and min_samples is low(Schubert et al., 2017).

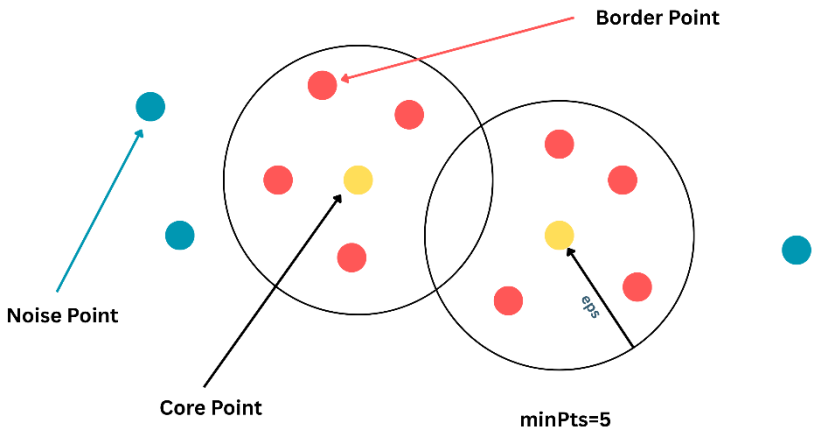

Fig. 1: Conceptual representation of DBSCAN

The original DBSCAN uses only linear memory because it has only two hyperparameters, making it easy to operate . This algorithm is robust to outliers and can detect an arbitrarily shaped cluster. This robust clustering algorithm in this research was designed to group points based on spatial density, making it particularly effective for spatial data such as landslide locations (latitude and longitude)(Birant & Kut, 2007). DBSCAN can identify clusters of arbitrary shapes and sizes while flagging points that do not belong to any cluster as noise. This study implemented the DBSCAN algorithm using scikit-learn (Virtanen et al., 2020). A clustering module was applied to systematically classify landslide occurrences into spatially coherent clusters. By leveraging DBSCAN's ability to detect irregularly shaped clusters and robustly identify noise, the algorithm was optimized with parameters eps=0.01 and min_samples=5 (Campello et al., 2013). This balance ensured that clusters captured meaningful geological and spatial patterns while isolating statistically insignificant outliers (labelled as -1), interpreted as noise points representing isolated or geomorphologically anomalous landslide events. The resulting clusters were plotted using density colour difference and the Virdis color scheme(Núñez et al., 2018). This approach improved the interpretability of the spatial dynamics of landslides and laid the

data-driven foundation (Reichenbach et al., 2018) for assessing environmental risk and geological connectivity.

DEEP LEARNING MODEL IMPLEMENTATION

Three deep learning architectures were implemented to develop landslide susceptibility maps for this research: Deep Neural Network (DNN), One-Dimensional Convolutional Neural Network (1D CNN), and Long Short-Term Memory (LSTM).

DNN is a popular approach to evaluating a range of natural hazards(Dahim et al., 2023). The specialized DNN architecture was developed to balance the complexity of the model layer with its ability to predict unseen data, a fundamental challenge for high-dimensional data such as geospatial features.

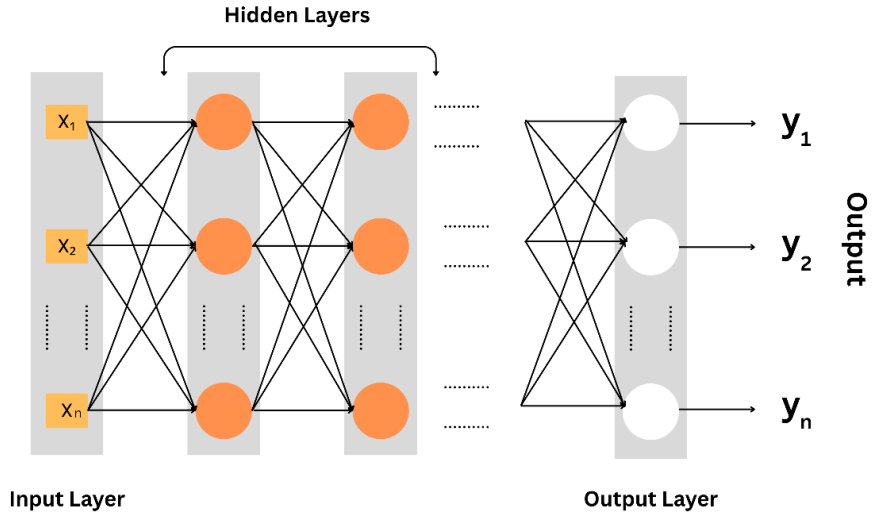

Fig. 2: General Architecture of DNN

The model uses a pyramidal topology (64→32→16 units) (LeCun et al., 2015a) and a progressively compressed stack of dense layers to achieve hierarchical feature abstraction through nonlinear transformations (Ghasemian et al., 2022). To capture nonlinear relationships accurately and efficiently, each layer uses the rectified linear unit (ReLU) activation (Dal Seno et al., 2024). The only limitation in intense networks, where gradual compaction is observed, was kept in check through model depth selection and initialization schemes. To mitigate the potential risk, a dual regularization framework, L2 regularization ($\lambda = 0.01$), was first applied to the kernel weights (He et al., 2015). Second, dropout layers (rate = 0.2) were interleaved between dense layers (Srivastava et al., 2014). This architecture ends with a single-output neuron with a sigmoid activation function that returns probabilistic outputs in the [0, 1] range for binary classification tasks. The ReLU activation function was chosen to validate training stability and convergence rate, and the structure of the pyramidal layer follows existing norms in parameter efficiency for geospatial applications. The model was trained using Adam as an optimizer (Kingma & Ba, 2017) and a DNN architecture; therefore, it is particularly effective in applications where simultaneous modelling of high-order feature interactions and spatial robustness is required (Reichstein et al., 2019)

CNN is the most powerful and significant algorithm in deep learning, with applications across 1D, 2D, and 3D data, and it belongs to different types of architectures. In this research, a 1D CNN (Kiranyaz et al., 2021), which is suitable for processing one-dimensional (1D) tabular data, was employed to predict the landslide susceptibility.

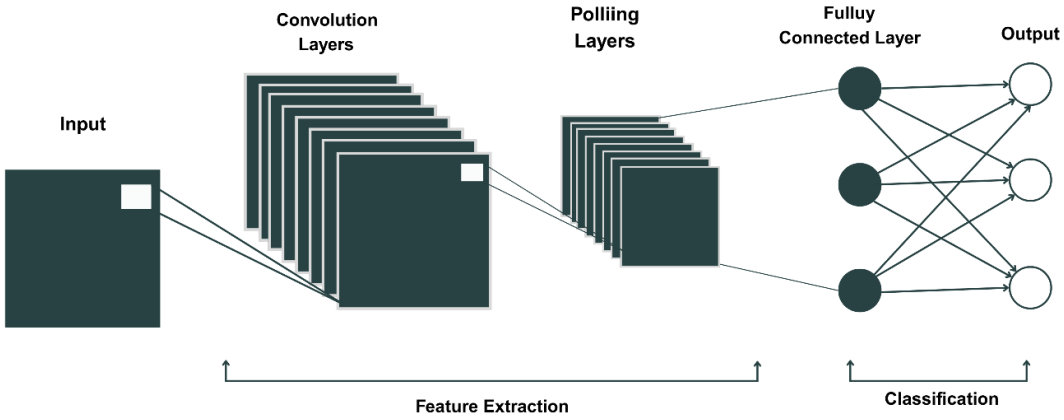

Fig. 3: A General Architecture of CNN

The 1D-CNN architecture was specifically designed to systematically account for spatial hierarchies in geospatial data. Such capability is useful for applications that require local parsing, e.g., landslide susceptibility mapping (Goodfellow et al., 2015b). The model begins with a 1D convolutional layer with 64 filters and a kernel size of 3 to capture spatial correlations between nearby points in the geographical output (Sameen et al., 2020a). The number of filters and the kernel size were adjusted to optimize sensitivity to micro-scale spatial structures, such as elevation changes. This model is particularly suitable for geospatial risk assessment, where interpretability of the outputs is important, and uncertainty quantification is desired. The algorithm was trained using the Adam optimization algorithm (Kingma & Ba, 2017).

Long Short-Term Memory (LSTM)

LSTM is a specialized type of Recurrent Neural Networks(RNNs), with a sophisticated architecture that mimics long-term dependency learning from data (Gers et al., 2000). To begin with, this algorithm was proposed in 1997 by (Hochreiter & Schmidhuber, 1997), and it has been successfully used in many deep-learning implementations and research on sequential data. The primary distinction between vanilla artificial neural networks and LSTMs is the collection of three gates—input gate, forget gate, and output gate—that an LSTM has to manage and safeguard information(Hussain et al., 2025).

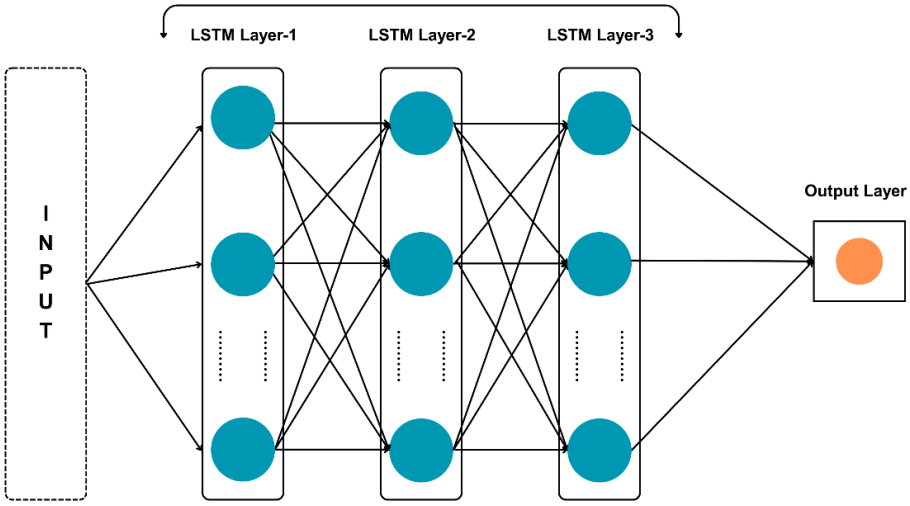

Fig. 4: A General Architecture of LSTM

The input gate notes how much new information needs to be created, the forget gate decides what information should be "forgotten" from the previous unit, and the output gate controls the state of the unit. This architecture employs a stacked Long Short-Term Memory (LSTM) to model sequential dependencies in the data. The network has two LSTM hierarchies, the first layer having 128 units and the second layer having 64 units. This cascaded design allows the model to learn temporal features in a hierarchical manner. The pyramidal design featuring dimensionality reduction per layer (128 → 64 → 32) balances effective representation learning with computational efficiency(Graves et al., 2013). The recurrent-dense hybrid architecture provides a strong foundation for capturing both sequential dependencies and nonlinear feature interactions. ReLU is well established for producing sparse activation in the hidden dense layers, thus improving generalization. Since we have a binary classification problem, a sigmoid activation function was used in the output layer. The model was implemented in TensorFlow/Keras and trained using backpropagation through time (BPTT) (Werbos, 1990) and gradient optimization with adaptive moment estimation (Adam) (Kingma & Ba, 2017).

LANDSLIDE SUSCEPTIBILITY MAPPING

Study Area

The study area for this research is the Rangamati Hill District in southeastern Bangladesh. Geographically, it lies between 22°27' and 23°44' north latitude and 91°56' and 92°33' east longitude (Hafsa et al., 2022). The state of Tripura borders this district to the north, Bandarban District to the south, Mizoram State of India and Chin State of Myanmar to the east, and Khagrachhari and Chattogram districts to the west. The geological setting of Rangamati is unique due to its position on the Arakan Yoma anticlinorium. The underlying strata primarily belong to the Bhuban Formation, which consists of light reddish-brown siltstone and shale. These formations are overlaid by the Bokabil Formation, composed of greyish-brown well-bedded siltstone and shale, prone to landslides. However, the bedrock and soil structure in these hills are unstable, contributing to

their susceptibility to landslides (Humayain & Biplob, 2021). Rangamati experiences a tropical monsoon climate characterized by intense rainfall during the monsoon season. The annual average rainfall is approximately 2673 mm, with 80% occurring during the monsoon season from June to September (Hafsa et al., 2022). A notable rainfall event occurred in June 2017, when approximately 510 mm of rain fell between June 12 and 14, triggering devastating landslides (Humayain & Biplob, 2021). Hydrological features, such as streams, rivers, and Kaptai Lake, significantly influence landslide occurrence in this region (Rabby et al., 2022). This comprehensive knowledge of Rangamati's geological setup, climatic conditions, topography, hydrology, and population distribution forms the basis for estimating landslide susceptibility in the study area. The location of the study area is outlined in the following figure:

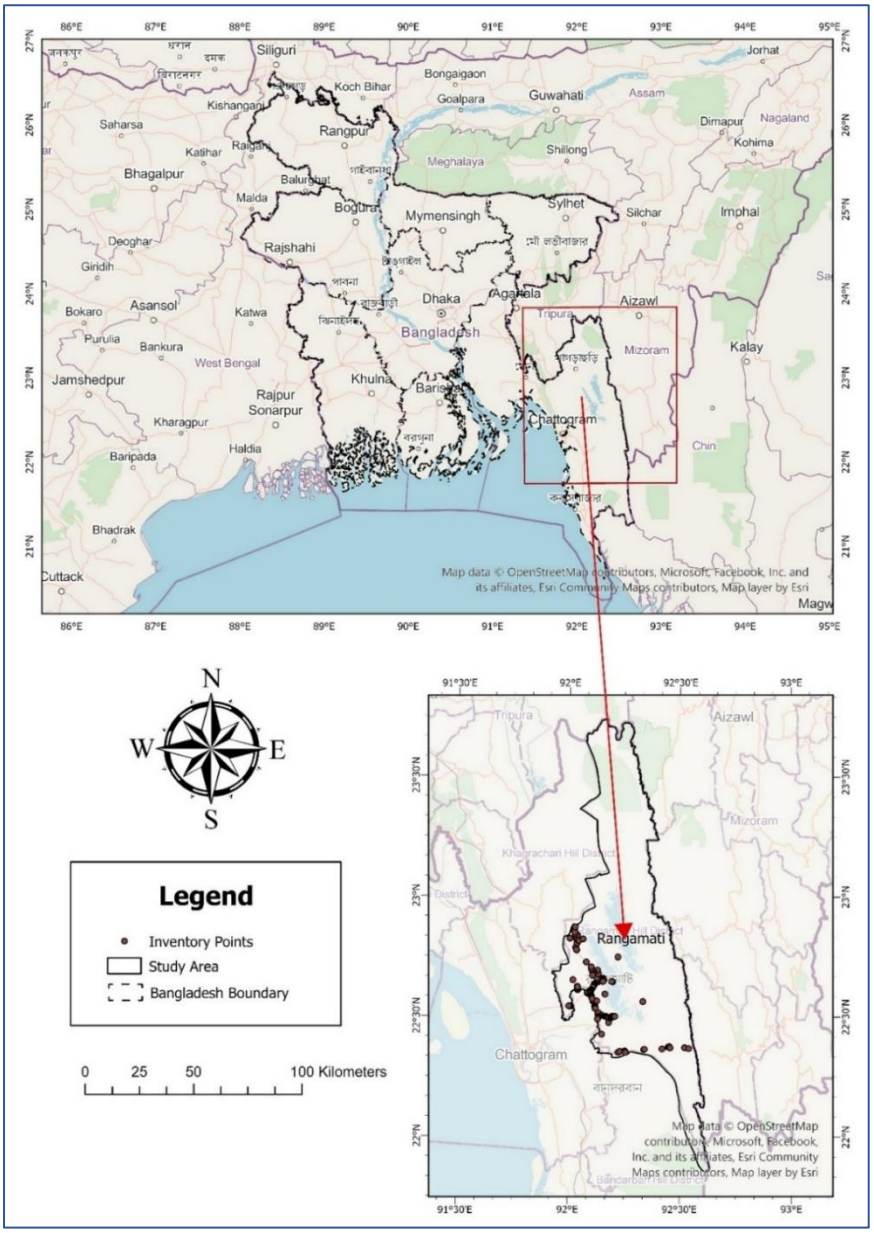

Fig. 5: Location of the research area. (a) Administrative boundaries of Bangladesh, (b) Rangamati Hill District with Landslides Inventory Points

Framework of Landslide Susceptibility Estimation

The research methodology used a systematic approach to address spatial sparsity and to implement deep learning models for landslide susceptibility mapping. The systematic approach is shown in the following figure:

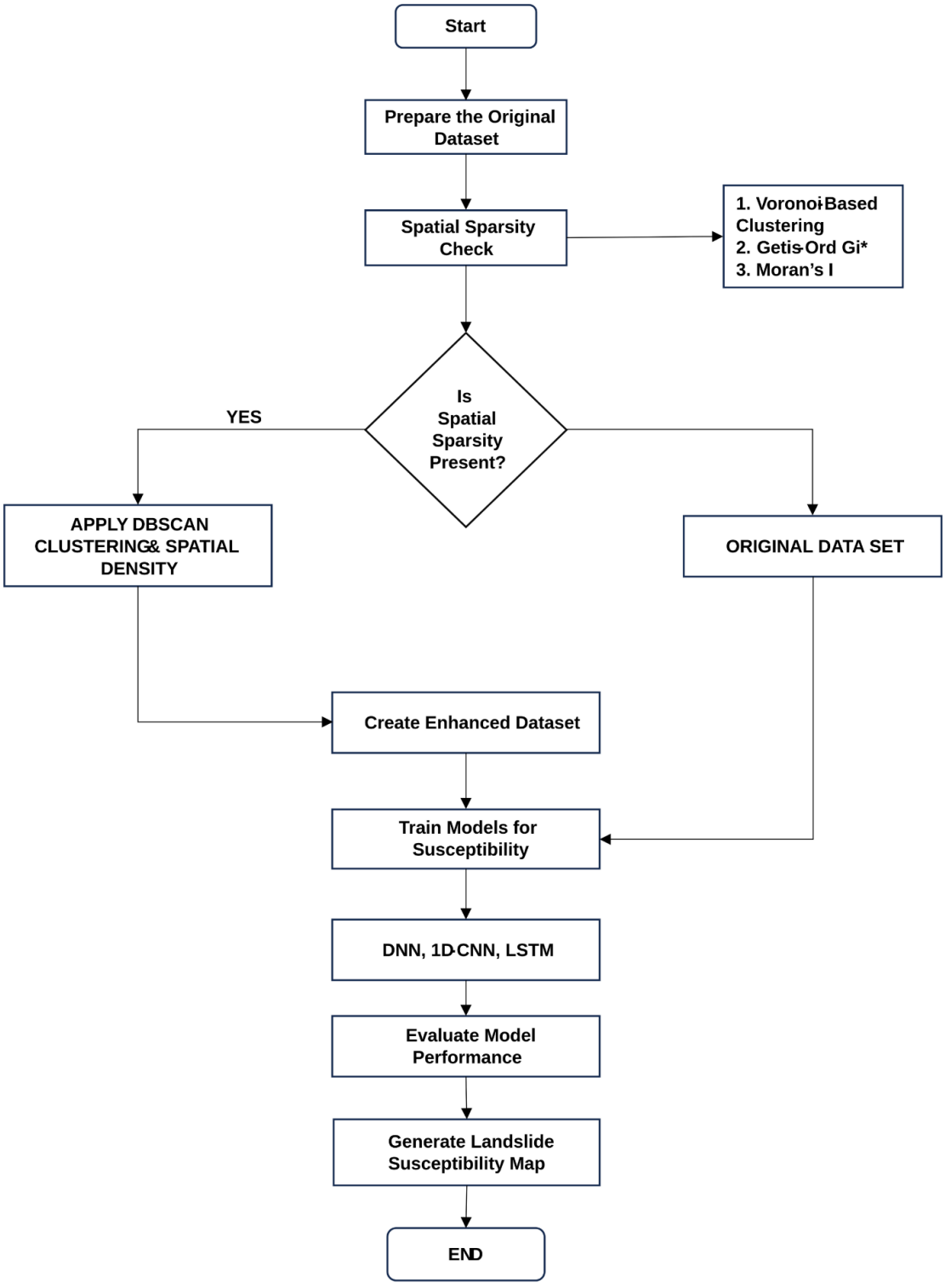

Fig. 6: Methodological Flowchart

Landslide Conditioning Factors (LCF)

The selection and quality of conditioning factors are crucial because they affect the performance of data mining techniques in landslide susceptibility analysis. A total of fourteen independent conditioning factors

comprising topographical parameters, hydrological indices, vegetation indicators, and environmental characteristics (Agrawal & Dixit, 2023) were selected for this study (Table 1). Digital Elevation Model with a 30-meter spatial resolution from (SRTM) was a primary data source for topographical and hydrological parameters (USGS, 2015). Using this DEM, eight layers for conditioning factors were extracted, which include elevation, slope, aspect, profile curvature, plan curvature, Stream Power Index (SPI), Topographic Wetness Index (TWI) and Terrain Ruggedness Index (TRI)(Hussain et al., 2025) (Fig. 2). Satellite data were used to compute vegetation index, the Normalized Difference Vegetation Index (NDVI) by pixel, using Sentinel-2 images (10-meter spatial resolution). Land Use/Land Cover (LULC) classification was derived from ESRI Sentinel-2 imagery processing(Mind'je et al., 2020), while soil texture data was acquired from the SoilGrids global database. Rainfall data and drainage network information were also incorporated into the analysis as critical hydrological factors.

Table 1 Landslide Conditioning Factors

Factor	Source of Data	Spatial Regulation (m)
Elevation	https://earthexplorer.usgs.gov/ SRTM DEM	30m x 30m
Slope	https://earthexplorer.usgs.gov/ SRTM DEM	30m x 30m
Aspect	https://earthexplorer.usgs.gov/ SRTM DEM	30m x 30m
Curvature	https://earthexplorer.usgs.gov/ SRTM DEM	30m x 30m
SPI	https://earthexplorer.usgs.gov/ SRTM DEM	30m x 30m
TWI	https://earthexplorer.usgs.gov/ SRTM DEM	30m x 30m
TRI	https://earthexplorer.usgs.gov/ SRTM DEM	30m x 30m
NDVI	https://earthexplorer.usgs.gov/ Landsat 8 level 2 imagery	10m x 10m
LULC	https://livingatlas.arcgis.com/landcover/ Esri | Sentinel-2 Land Cover	10m x 10m
Rainfall	https://crudata.uea.ac.uk/cru/data/hrg/	
Distance to Drainage	https://earthexplorer.usgs.gov/ SRTM DEM	30m x 30m
Soil Texture	https://soilgrids.org/ ISRIC (International Soil Reference and Information Centre)	250-meter resolution

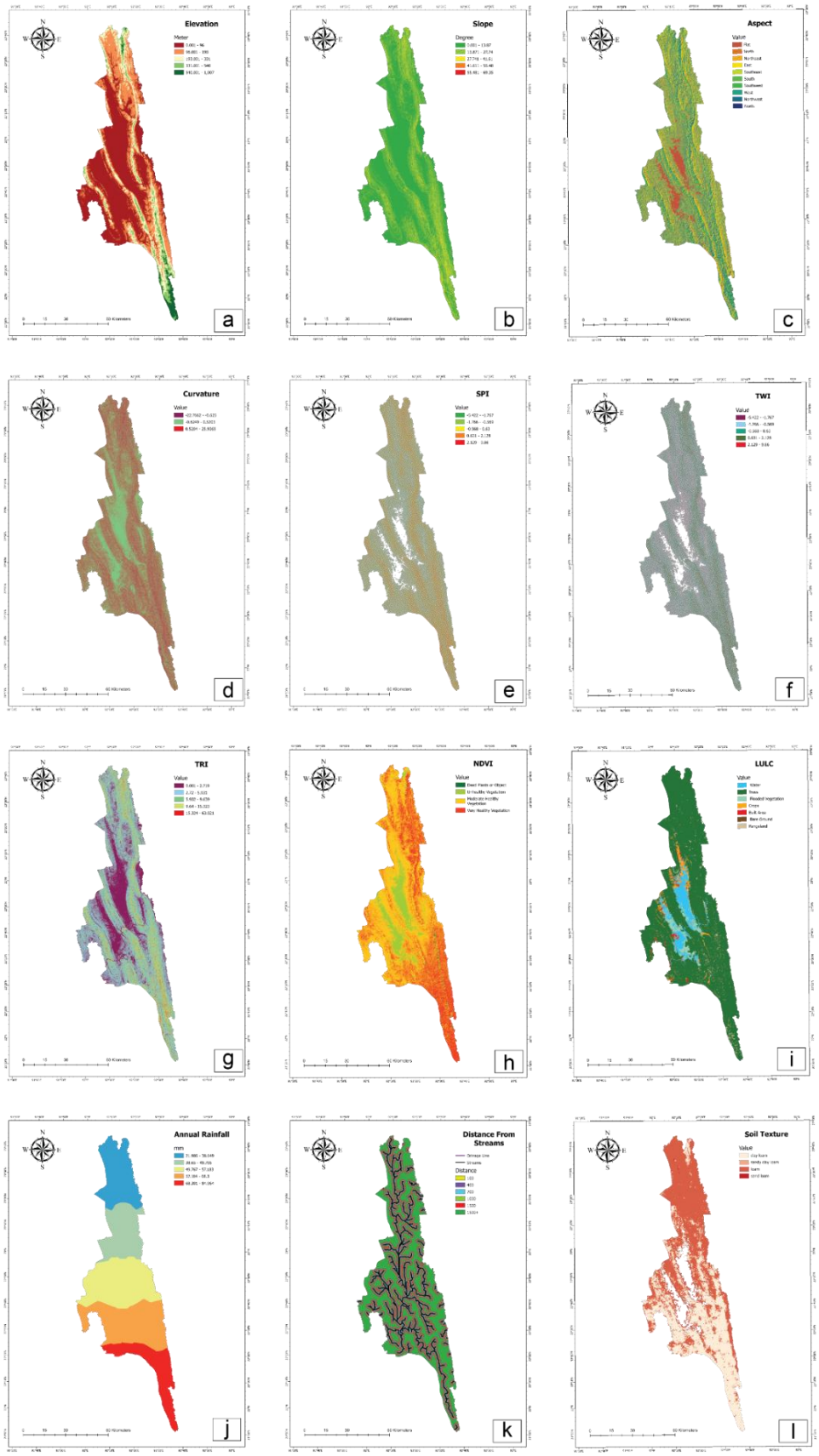

Fig. 7: Landslide conditioning factors in the research area: (a) Elevation, (b) Slope, (c) Aspect, (d) Curvature, (e) SPI, (f) TWI, (g) TRI, (h) NDVI, (i) LULC, (j) Rainfall, (k) Distance from drainage, (l) Soil texture

Landslide Inventory Map

The landslide inventory map is the first step in this research. Historical landslide points were collected from NASA data, CEGIS (a GIS organization in Bangladesh), the Bangladesh Army, and other sources, yielding 198 points. The points correspond to locations with varying topographical conditions in the Rangamati District. They were used as location points to process as point features using the GIS environment on an inventory map suitable for analyzing landslide occurrences. This map provides critical insights into previously landslide-prone areas in the Rangamati Hill District.

RESULTS

Spatial Sparsity Analysis

The spatial sparsity analysis in Step 1 indicated an uneven distribution in the landslide dataset. The Voronoi diagram (Fig. 8) illustrates significant variation in cell sizes across the study area, with larger polygons indicating sparse data regions and smaller cells indicating higher data density. This diagram partitions the spatial domain into polygons that represent the area closest to a specific data point. The blue lines define the boundaries, each equidistant from its neighbors. Notably, the Voronoi diagram highlighted sparse regions with larger polygons, particularly in the southern and southeastern areas and along parts of the eastern margins. At the same time, dense clusters are mainly visible in the central-western and parts of the northeastern regions, where smaller polygons predominate. Large polygons in sparse areas suggest inadequate spatial coverage, which can introduce bias in modeling by underrepresenting certain regions. Conversely, dense clusters may overemphasize specific geographic features, potentially distorting model predictions if not balanced. This visual assessment is a preliminary indication of spatial sparsity, emphasizing the need for mitigation.

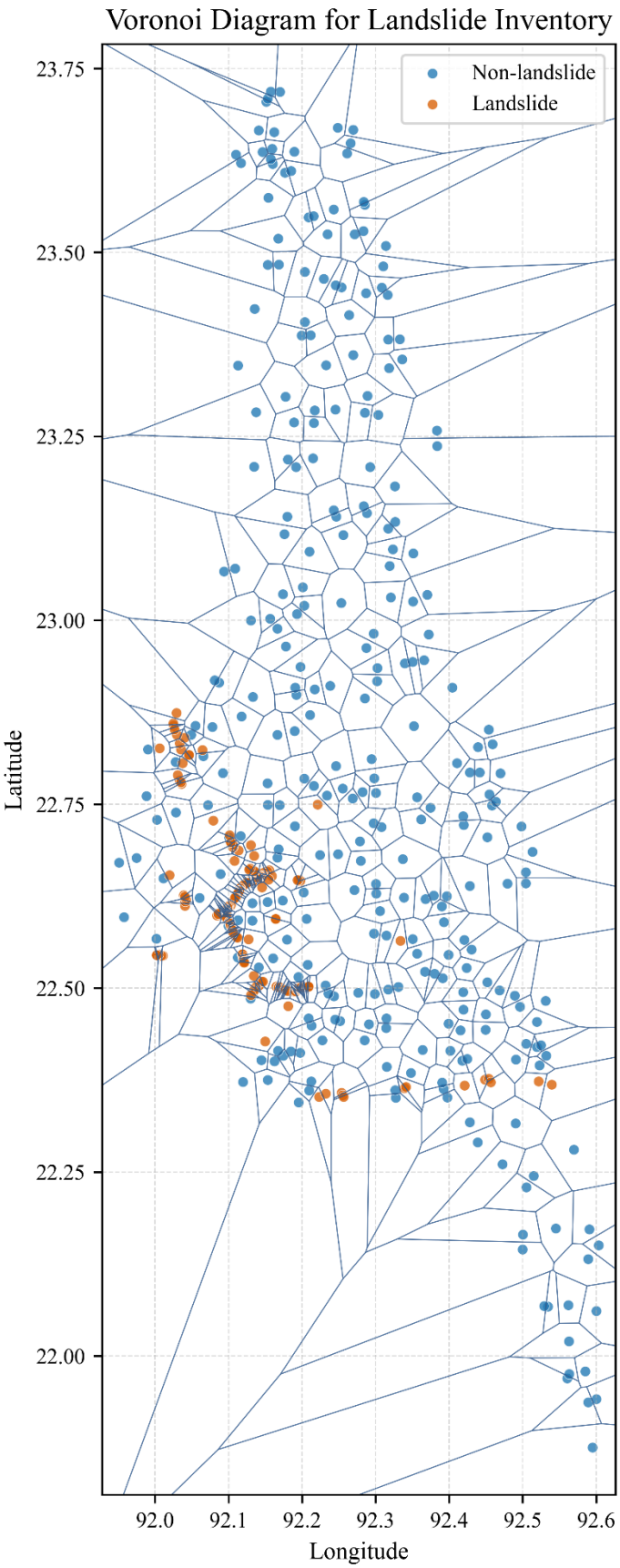

Fig. 8: Voronoi Diagram

To statistically validate spatial sparsity in the landslide dataset, the Getis-Ord Gi* statistic was used to quantify local spatial autocorrelation. The analysis revealed nine isolated spatial units (IDs: 198, 218, 220, 302, 379, 388, 408, 448, 457) lacking adjacent relationships. These units, classified as spatial "islands," exhibit no neighboring observations, highlighting inherent data gaps and heterogeneity in spatial coverage. The computed Gi* Z-scores for the first ten spatial units ranged from 0.491 to 1.085, with a mean of 0.852 ± 0.215. Indices 4–9 notably exhibited Z-scores exceeding 1.0 (e.g., 1.085 at index 4), indicating localized clustering tendencies in specific regions. However, the marginal statistical significance ($p > 0.05$ for all units) reinforces the prevalence of sparse data distributions. The combination of non-significant clustering signals and topological discontinuities underscores the necessity of sparsity-aware modelling frameworks to mitigate biases in subsequent geospatial analyses. The accompanying spatial analysis map in Fig. 9 (based on Getis-Ord Gi* Z-scores) illustrates clustering patterns. Hotspots (red regions) indicate statistically significant clustering of high values, predominantly between latitudes 22.5–22.75 and longitudes 92.0–92.2. Conversely, cold spots (blue regions) represent clusters of low values, mainly in the northern and southern extremes of the study area. Neutral or white areas, with Z-scores near zero, signify regions with no significant clustering. This analysis confirms spatial sparsity in the dataset, necessitating targeted interventions to improve geospatial modeling accuracy.

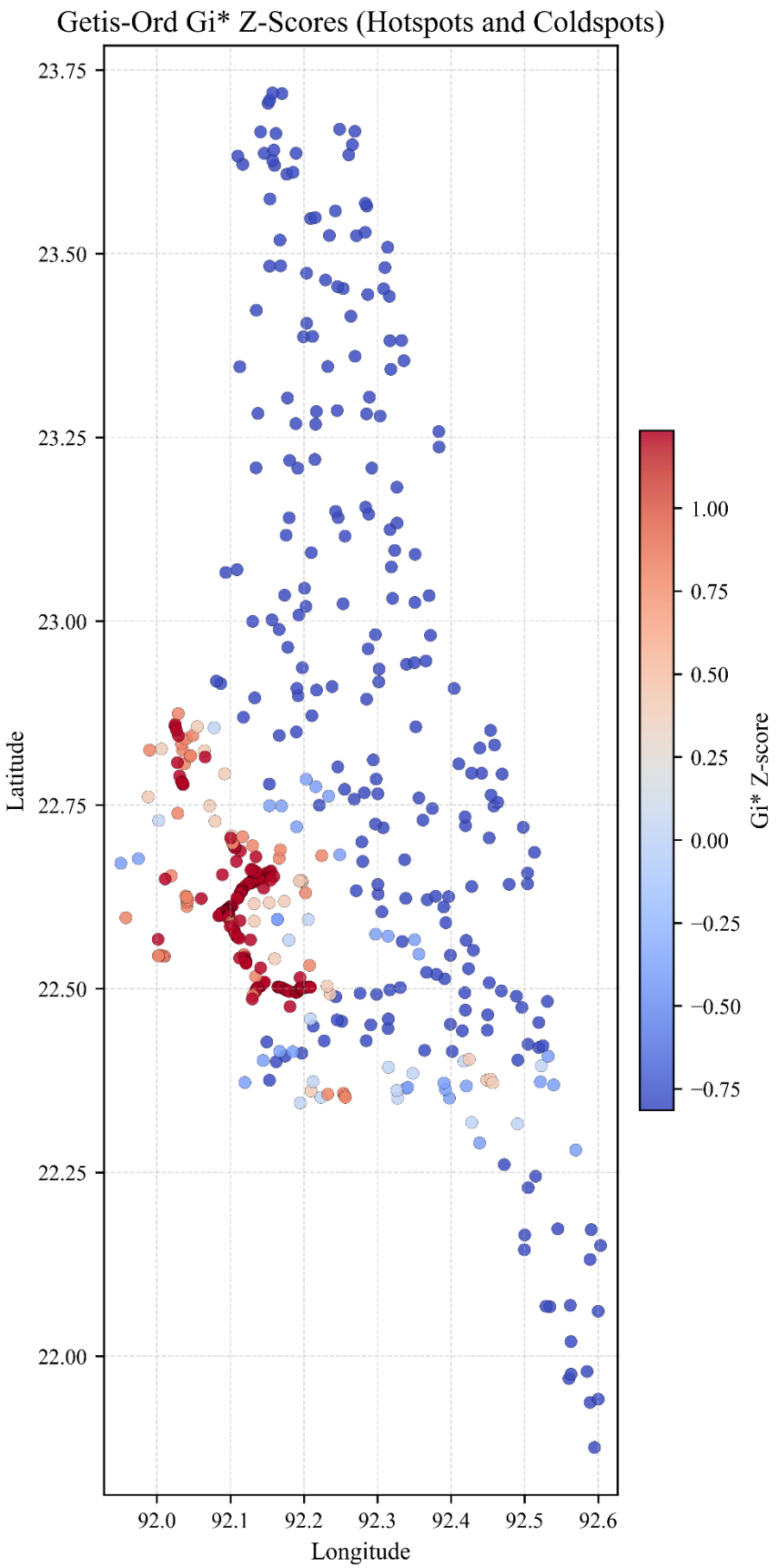

Fig. 9: Getis-ord Gi*

The global spatial autocorrelation analysis using Moran's I produced a value of 0.7258 with a pseudo p-value o.oo1, indicating a strong positive spatial autocorrelation in the landslide dataset. This suggests that areas with high landslide occurrence tend to be surrounded by other high-occurrence areas, whereas regions with low occurrence are similarly clustered. Such spatial dependence reflects the presence of geographically coherent patterns rather than a purely Gaussian distribution.

Moran's I scatter plots in Fig. 10 visually reinforce feature values against their spatially lagged counterparts. The positively sloped regression line further demonstrates the spatial dependence exponents. The four quadrants, divided by the mean of the feature and lagged values, reveal local association patterns. The patterns are most prominently high-high clusters in the upper right quadrants and low–low clusters in the lower left, alongside a few high-low and low–high outliers. Overall, the analysis provides clear evidence of strong spatial clustering and non-random spatial organization in the dataset.

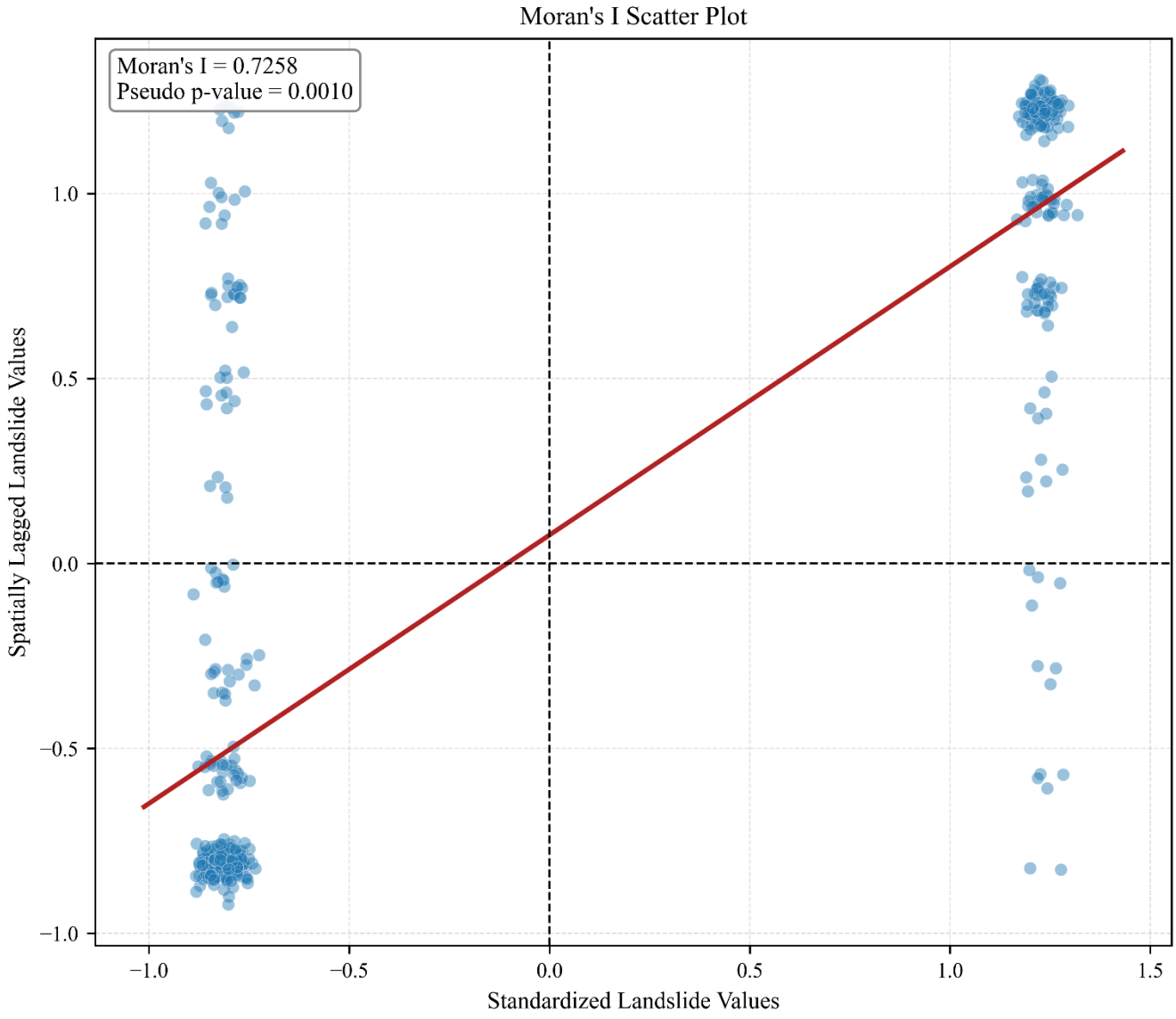

Fig. 10: Moran's I Scatter Plot

Spatial Sparsity Mitigation

The application of DBSCAN clustering and spatial density analysis significantly improved the quality and spatial representation of the dataset for landslide susceptibility mapping. As illustrated in Fig. 11, DBSCAN successfully identified clusters based on spatial proximity and density, assigning unique cluster IDs (0–8) to regions with sufficient data density while labelling sparse points as noise (-1). The clustering results showed a substantial number of noise points distributed throughout the study area, stemming from the spatial sparsity of the original dataset. Conversely, DBSCAN emphasized highly clustered regions, which are crucial for gaining insights into the spatial distribution of landslide-prone areas. Spatial density analysis further augmented the dataset, categorizing clusters into sparse and dense regions, with metric-specific denser organisms over-represented. Sparse clusters were defined by identifiers [-1, 0, 1, 6, 5, 7, 3, 4, 2, 8], providing a quantitative and systematic measure of sparsity distribution across the study area. This classification provided important spatial context by identifying which areas were sparse and which were not.

To mitigate spatial sparsity, we enhanced the original 12-factor conditioning dataset by deriving spatial context features from coordinates (Latitude, Longitude). Specifically, DBSCAN (eps=0.01, min_samples=5) was applied to generate a categorical **Cluster** label (including -1 for noise), and a density-threshold rule was used to derive a binary **Sparse_Cluster** indicator for points in low-density clusters. Thus, the enhanced table consists of the original conditioning factors with these DBSCAN-based spatial variables. In the final deep-learning experiments, **Cluster** was used as the added predictor in the enhanced dataset.

Added-feature table:

Added variable	Type	How computed	Used in final DNN/CNN/LSTM comparison?
Cluster	Integer categorical	DBSCAN on (Longitude, Latitude) with eps=0.01, min_samples=5; -1 = noise	Yes
Sparse_Cluster	Binary (0/1)	Cluster density rule: cluster marked sparse if cluster_count < 0.2 * avg_density * N	No (used in sparsity analysis/feature exploration)

These refinements overcome the limitations in the original dataset by complementarily capturing spatial sparsity and density variations. This is a potential benefit for deep learning models, as they gain additional features that enable them to learn spatial patterns and distinguish areas susceptible to landslides. Specifically, sparse regions can be handled differently during model training to reduce bias from uneven data distribution. Furthermore, these improvements enhance interpretability by allowing susceptibility predictions to be analyzed within the context of spatial clustering and density. Overall, integrating DBSCAN clustering and

spatial density analysis resolved the sparsity issue and added valuable spatial information to the dataset. This enriched dataset yielded more accurate landslide susceptibility maps and better model performance than the original dataset.

.

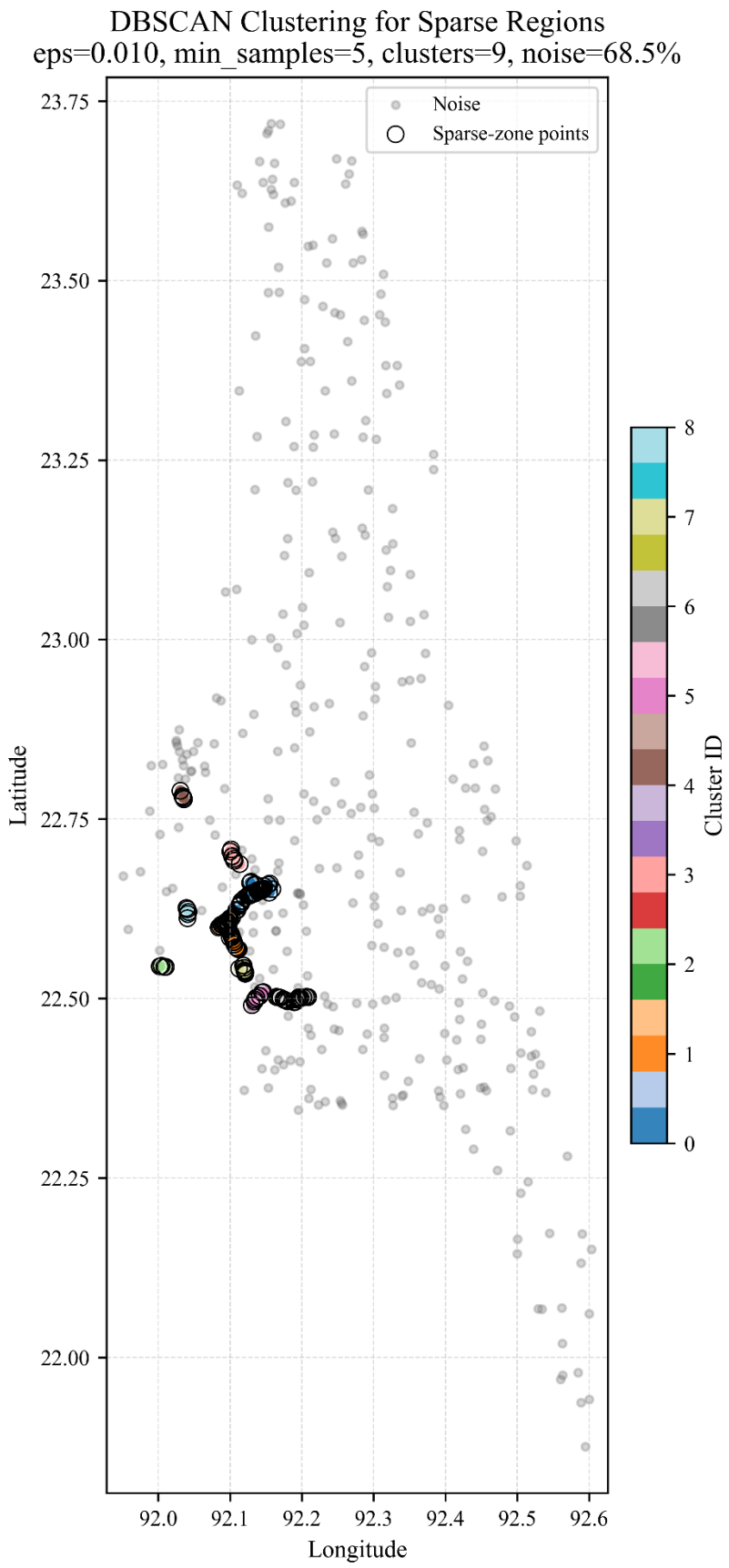

Fig. 11: DBSCAN clustering for Sparse Region

Deep Learning Model Performance

To explicitly test the value of sparsity mitigation, the original dataset was used as a baseline, and DNN, 1D-CNN, and LSTM were compared on both original and enhanced inputs. The enhanced 1D-CNN achieved the best overall performance (AUC = 0.9633, accuracy = 0.92, precision = 0.9211, recall = 0.8750, F1 = 0.8974), improving over the original 1D-CNN (AUC = 0.9442, accuracy = 0.89, precision = 0.8537, recall = 0.8750, F1 = 0.8642). Enhanced LSTM also improved substantially (AUC 0.9525 vs 0.9142; F1 0.8462 vs 0.7750), whereas DNN showed mixed behavior, indicating that sparsity-mitigation benefits are architecture-dependent. Therefore, the final susceptibility map was produced using the enhanced 1D-CNN, as it provides the best balance between discrimination power and precision-recall performance for practical hazard zoning.

Using DNN, 1D CNN, and LSTM models in TensorFlow and Keras, detailed results showed that encouraging spatial sparsity strengthened the models. The performance metrics for all models are provided in Table 2.

Table 2 Model Accuracy Metrics

Model	AUC	Train Accuracy	Test Accuracy	Precision	Recall	F1 Score
Enhanced_Dataset_DNN	0.96	0.919	0.87	0.909	0.75	0.821
Enhanced_Dataset_1D CNN	**0.962**	**0.896**	**0.89**	**0.914**	**0.8**	**0.853**
Enhanced_Dataset_LSTM	0.955	0.937	0.89	0.939	0.775	0.849
Original_Data_DNN	0.940	0.871	0.9	0.875	0.875	0.875
Original_Data_1D CNN	0.937	0.874	0.9	0.840	0.925	0.880
Original_Data_LSTM	0.927	0.884	0.81	0.8	0.7	0.746

The sparsity-free dataset demonstrated significant improvements for specific architectures. Figure 12 presents a comparative analysis of the ROC curves, which provides insight into the models' discrimination abilities. The proximity of the 1D-CNN curve to the top-left corner confirms its superior ability to balance sensitivity and specificity. However, the overlap among several curves in the high-specificity region suggests that model selection should consider application-specific requirements rather than relying solely on AUC values.

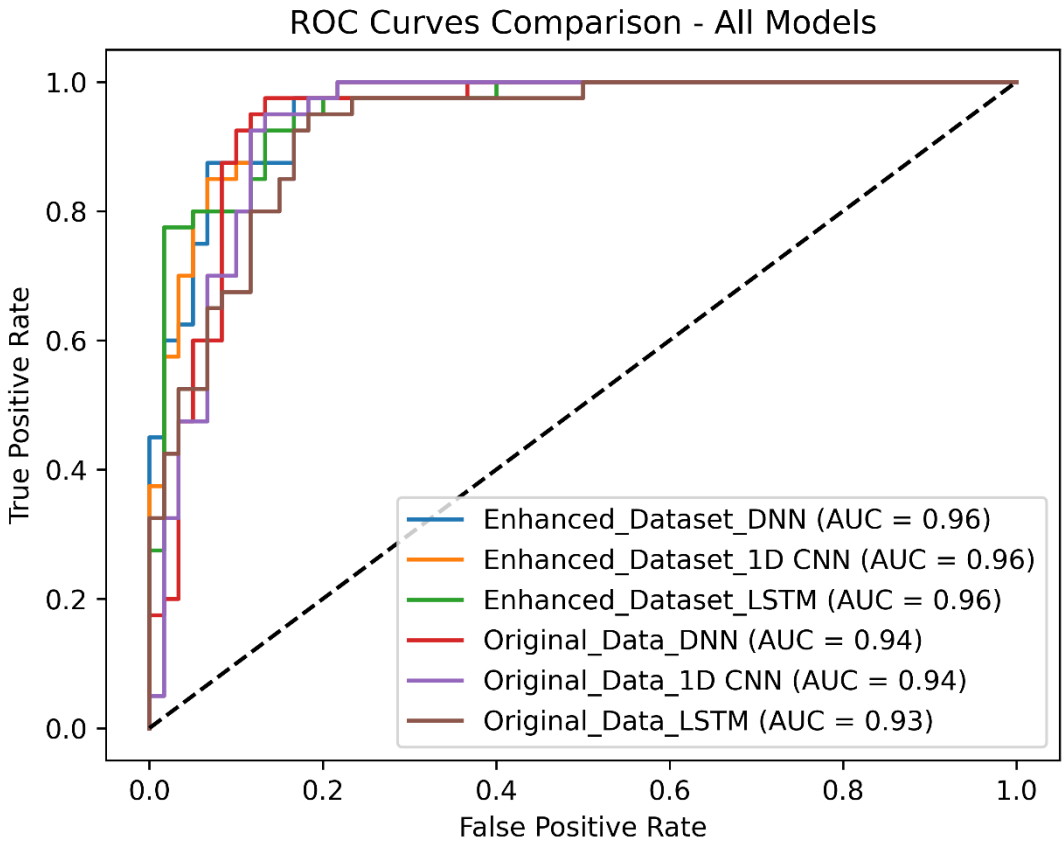

Fig. 12: The receiver operating characteristics (ROC) curves and AUC values of all models.

The discrepancy between training and test accuracies warrants attention. The LSTM model on the enhanced dataset showed the largest gap (0.937 vs. 0.89), which may indicate some overfitting despite its strong overall performance. The DNN and 1D-CNN models on the original dataset showed the smallest gaps, suggesting better generalization capabilities on unmodified data.

A critical observation is the consistent trade-off between precision and recall across all models. The LSTM model on the enhanced dataset achieved the highest precision (0.939) but at the cost of lower recall (0.775), indicating excellent optimistic prediction accuracy but potentially missing some positive cases. Conversely, the 1D-CNN on the original dataset showed the highest recall (0.925) but with reduced precision (0.840), suggesting it captured more positive cases but with more false positives.

The radar plots in Fig. 13 reveal that no single model dominates all performance dimensions. This multifaceted evaluation highlights the importance of selecting models based on specific application requirements rather than relying on any single metric.

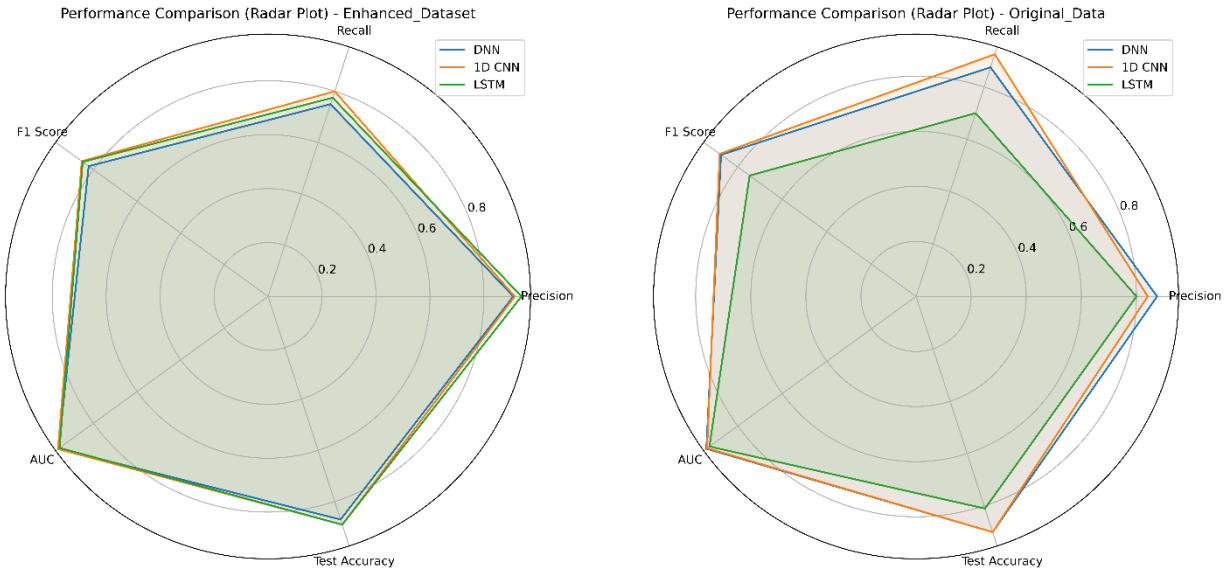

Fig. 13: Evaluation metrics of all models: (a) Enhanced dataset, (b) Original dataset

Overall, the 1D-CNN model applied to the sparsity-free dataset performed the most balanced, achieving the highest AUC (0.962) and an optimal precision-recall trade-off. This superior performance can be attributed to the ability of the model to capture spatial patterns through its convolutional architecture, further enhanced by the sparsity mitigation process, which provides spatial context.

SHAP-Based Feature Importance and Model Interpretability

The SHAP-based feature importance analysis revealed significant insights into the factors driving landslide susceptibility in the Rangamati District. Figure 14 (a) presents the SHAP summary plot for the original dataset, while Figure 14 (b) shows the results for the enhanced sparsity-mitigated dataset (using the best model 1d cnn). In the original dataset analysis, NDVI was the most influential factor for landslide prediction, with the largest SHAP value range. This finding supports the established understanding of vegetation's role in slope stability. The analysis of the sparsity-mitigated dataset revealed a dramatic shift in feature-importance rankings, with spatial-context features emerging as the primary predictors. The Cluster feature derived from DBSCAN demonstrated the highest importance, with its SHAP values showing a spread distribution range, indicating its great influence on model predictions.

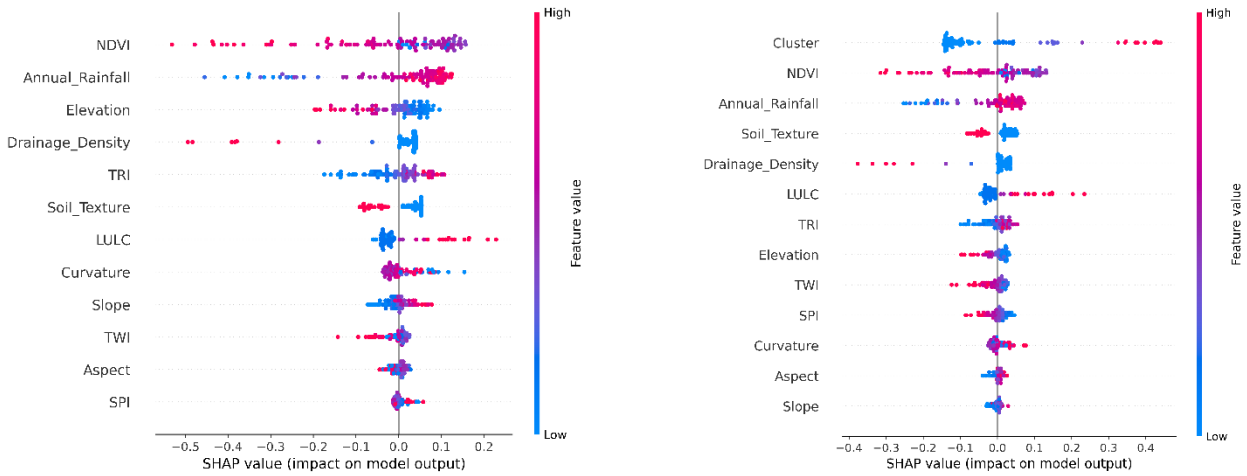

Fig. 15: SHAP features importance in (a) orginal dataset, (b) enhanced dataset

This finding of the study confirms that spatial clustering patterns captured through the DBSCAN algorithm effectively encode critical information about landslide susceptibility that was previously missing in the original dataset. The enhanced dataset confirms that addressing spatial sparsity provides vital insights that were previously unavailable to the original dataset. This spatial context allows the model to better understand the heterogeneous nature of landslide susceptibility across the study area, leading to more accurate predictions. Traditional conditioning factors maintained their physical relevance across both datasets, but their relative importance shifted when spatial context was introduced. This finding suggests that while environmental factors like NDVI, rainfall, and topography remain fundamental to landslide processes, the spatial arrangement and clustering patterns of these factors provide additional predictive power that enhances overall model performance.

LANDSLIDE SUSCEPTIBILITY MAP

Based on the performance evaluation, the 1D-CNN model trained on the sparsity-free dataset was selected to generate the final landslide susceptibility map for the Rangamati District. The susceptibility values were interpolated across the study area to create a continuous surface representing the spatial distribution of landslide probability. The northern portion of Rangamati District predominantly exhibits Very Low to Low

susceptibility (dark green to light green areas), indicating relatively stable terrain conditions. This pattern gradually transitions to medium susceptibility (yellow zones) in the central regions, suggesting moderate landslide risk in these transitional landscapes. The southern section of the district presents the most concerning scenario, with extensive High (orange) and Very High (red) susceptibility zones. These critical areas are notably concentrated in the southwestern and south-central regions, where the highest density of inventory points (black dots) is also observed. This strong spatial correlation between documented landslide locations and predicted high-risk zones validates the model's effectiveness in identifying vulnerable areas. The distribution pattern aligns with the expected influence of topographic, geological, and hydrological factors mentioned in the preliminary analysis. The transparent north-south gradient of increasing susceptibility suggests a systematic variation in underlying environmental conditions across the district. The southwestern region appears particularly vulnerable, with the most extensive contiguous areas of Very High susceptibility. The patchy distribution of susceptibility classes in the central region, with interspersed Medium, Low, and High susceptibility zones, reflects the complex interplay of local factors influencing landslide potential. This heterogeneity highlighted the importance of high-resolution analysis for effective risk management at the regional scale.

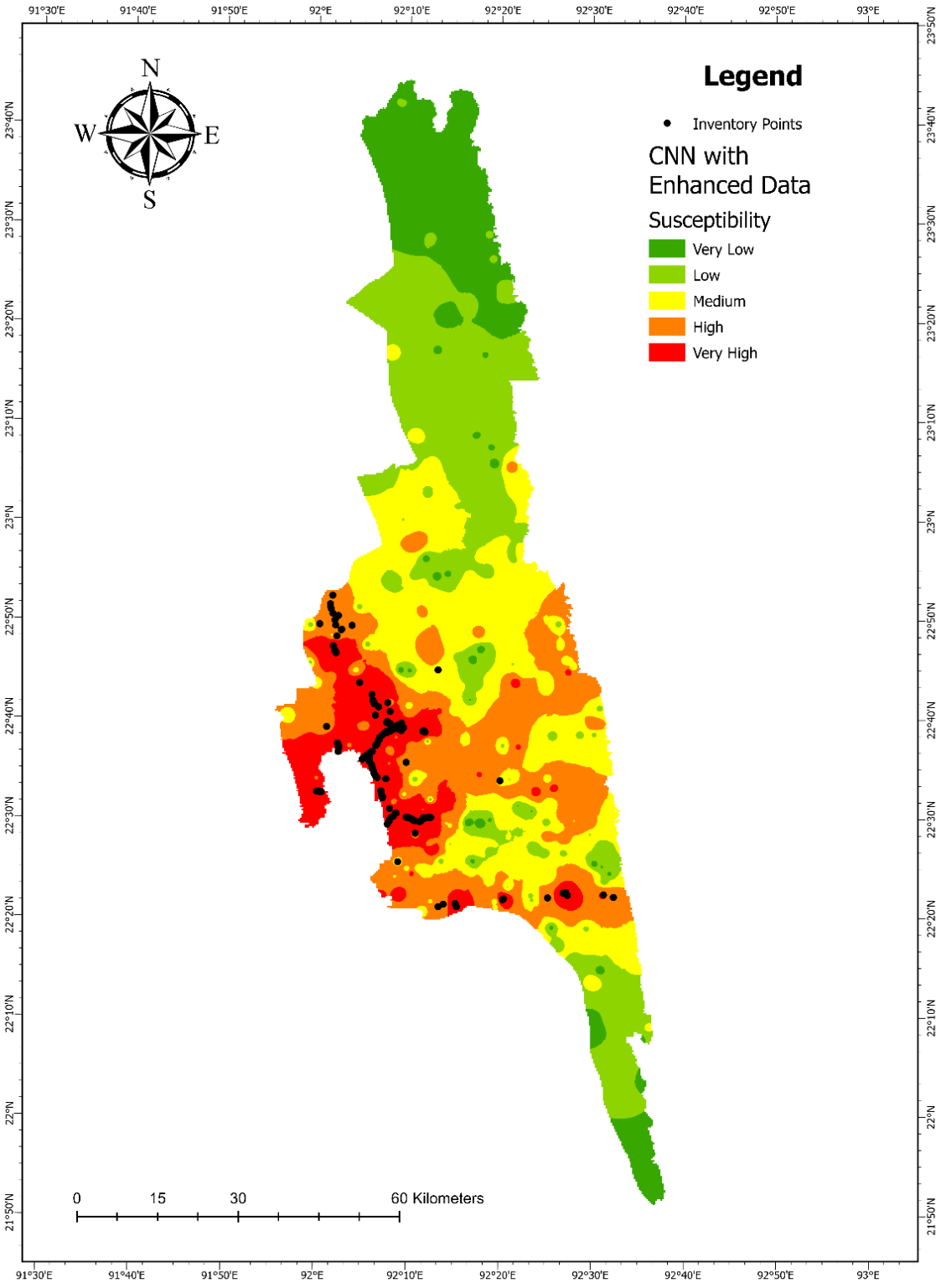

Fig. 16: Landslide Susceptibility Map

The map provides crucial spatial information for prioritizing risk reduction interventions, with a clear delineation of the most vulnerable areas requiring immediate attention from disaster management authorities. The susceptibility gradient from north to south also provides insights into the underlying geomorphological and climatic factors that drive landslide risk in the Rangamati District.

DISCUSSION

This study makes a significant contribution by explicitly addressing the challenge of spatial sparsity in landslide data, which is often overlooked in susceptibility modelling, especially in underdeveloped or developing countries. The first Step confirmed the uneven spatial distribution of the landslide dataset with several complementary spatial sparsity checks. Voronoi analysis visually showed the data density throughout the study area, the Getis-Ord Gi* statistic exposed isolated points, and Moran's I value (0.7258) reflected moderate to strong spatial clustering, thus providing evidence that sparsity mitigation strategies should, if possible, be employed. This new approach, a robust judgment to quantifying spatial sparsity, is a step forward from previous studies that often ignore this spatial sparsity issue(Aristizábal et al., 2025). In the next step, the DBSCAN clustering identified sparse regions in the landslide data set and provided an enhanced dataset with spatial context (Cluster) . This procedure introduces cluster information as a new feature in the dataset to address spatial heterogeneity in environmental modelling. Examining the performance of model metrics learned on original versus sparsity-mitigated datasets is intriguing. The best overall AUC of 96.25% was achieved by the enhanced dataset in 1D CNN, followed by the enhanced dataset in DNN with 96%, and the enhanced dataset in LSTM with 95%. The superiority of 1D-CNN aligns with its ability to capture spatial patterns in geohazards(Sameen et al., 2020). The performance of the 1D-CNN architecture is consistent with results from recent studies demonstrating the effectiveness of CNN in capturing spatial patterns for geohazard assessment. Notably, the LSTM model showed the most dramatic improvement, with AUC increasing from 0.927083333 to 0.9554166671. This suggests that sequential models particularly benefit from improved spatial representation, possibly because they can better capture the sequential relationships between conditioning factors when spatial context is adequately represented.

The integration of SHAP analysis in this study addressed one of the most critical limitations of deep learning models in geohazard assessment: the lack of interpretability (Indra Prakash et al., 2024). Unlike traditional "black box" machine learning approaches, the SHAP framework provides quantifiable explanations for how each conditioning factor contributes to landslide susceptibility predictions, enabling stakeholders to understand and trust model decisions (Xiao et al., 2024). The SHAP analysis provided compelling evidence for the effectiveness of the spatial sparsity mitigation approach. The emergence of spatial context features (Cluster) as top predictors in the enhanced dataset confirms that addressing spatial heterogeneity captures previously hidden patterns in landslide susceptibility(Lu et al., 2023). This finding validated the theoretical foundation that spatial clustering patterns encode critical geomorphological information that traditional conditioning factors alone cannot fully represent.

This research approach represents a novel methodological contribution to landslide susceptibility mapping. Unlike conventional methods that might discard or spatially sparse regions, the framework transforms sparsity information into valuable predictive features. This approach addresses a fundamental challenge in geospatial modelling where data collection is often constrained by accessibility, cost, or technical limitations. The landslide susceptibility maps generated from the best-performing model provide crucial information for risk management in Rangamati District. The high-precision values achieved by enhanced dataset models

enable authorities to confidently prioritize high-risk areas for intervention, thereby optimizing resource allocation for mitigation measures.

Despite the promising results, several limitations should be acknowledged. First, while our sparsity mitigation approach improves model performance, it does not substitute for comprehensive field surveys and expanded data collection. Future work should validate our predictions with additional ground-truth observations, particularly in areas identified as sparse(Yu et al., 2025).Second, our models rely primarily on static conditioning factors, whereas landslide susceptibility is dynamic and influenced by temporal variables like precipitation intensity and duration. Future research could integrate real-time monitoring data to develop early warning systems that dynamically update susceptibility predictions during critical rainfall events.

Future work has various potential research directions. Transfer learning may allow us to fine-tune our models for nearby regions with similar geology but fewer landslide inventory records. Investigating more sophisticated architectures, such as attention mechanisms or Graph Neural Networks, is likely to enhance predictive power by explicitly modeling complex spatial relationships (Huang et al., 2020). Furthermore, multi-temporal analysis considering variations in land use and climate could help understand changes in landslide susceptibility in the area.

This study demonstrates that addressing spatial sparsity positively impacts the use of deep learning methods for landslide susceptibility mapping. The 1D-CNN model, with spatially improved data, achieved the highest prediction accuracy, making it the best model for use in the same geological context. The methodology presented in this study provides an excellent working model for future landslide susceptibility estimation in similar settings, where data availability is spatially non-uniform. By converting an inherent limitation of typical data into an informative feature, our method contributes to the development of geohazard assessment and landslide risk management.

CONCLUSION

This study introduces a novel methodological framework that combines spatial sparsity mitigation with deep learning to enhance landslide susceptibility mapping. Using Voronoi-based clustering, Getis-Ord Gi* analysis, and Moran's I, spatial sparseness in landslide data was quantified and subsequently addressed by applying DBSCAN clustering to enrich the dataset with spatial context features, which eventually emerged as critical predictors in predictive modeling. Rangamati, the largest hilly district, was selected as a case study to substantiate the methodological framework. Given the very limited landslide inventory data, which is crucial for susceptibility prediction, sparsity was evaluated and addressed to enhance the inventory dataset for more reliable prediction of landslide susceptibility. Three deep learning models were considered, and among them, the 1D-CNN model trained on the sparsity-mitigated dataset demonstrated superior performance, achieving an AUC of 0.9625 and an F1-score of 0.853. The integration of SHAP analysis with spatial sparsity mitigation and deep learning significantly advances landslide susceptibility mapping methodologies. The SHAP framework provided unprecedented insights into model decision-making processes, revealing that spatial

context features derived from clustering analysis encode critical information about landslide susceptibility patterns that traditional conditioning factors cannot fully capture. At the same time, the final susceptibility map identified high-risk zones concentrated in southern Rangamati, consistent with historical landslide occurrences and steep, monsoon-affected terrain. This research contributes to the field by providing a robust framework that can be adapted to other regions facing similar spatial sparsity challenges. From a policy perspective, the high-resolution susceptibility map provides actionable insights for prioritizing land-use regulations, infrastructure reinforcement, and emergency preparedness in high-risk areas. Micro-zoning strategies and community awareness programs, informed by these findings, could improve disaster resilience, while collaboration between researchers and policymakers can ensure adaptive strategies align with sustainable development goals. By transforming spatial sparsity into an actionable feature, this framework offers a replicable template for landslide-prone regions globally, bridging data limitations with innovative modelling to foster safer, more resilient communities. Despite these advancements, the study is constrained by reliance on a limited landslide inventory and static conditioning factors that overlook dynamic triggers such as real-time rainfall. Future studies could explore more complex deep learning architectures and higher-resolution datasets to further enhance the accuracy of landslide susceptibility mapping.

DECLARATIONS

Funding

No funding was received for conducting this study

Competing interests / Competing financial & non-financial interests

The authors declare that they have no competing interests to disclose.

References

Andronov, L., Orlov, I., Lutz, Y., Vonesch, J.-L., & Klaholz, B. P. (2016). ClusterViSu, a method for clustering of protein complexes by Voronoi tessellation in super-resolution microscopy. *Scientific Reports*, *6*(1), 24084. https://doi.org/10.1038/srep24084

Anselin, L. (1995). Local Indicators of Spatial Association—LISA. *Geographical Analysis*, *27*(2), 93–115. https://doi.org/10.1111/j.1538-4632.1995.tb00338.x

Aristizábal, E., Lombardo, L., & Korup, O. (2025). *Spatial regression models to estimate landslide susceptibility*. SSRN. https://doi.org/10.2139/ssrn.5458364

Birant, D., & Kut, A. (2007). ST-DBSCAN: An algorithm for clustering spatial–temporal data. *Data & Knowledge Engineering, Intelligent Data Mining*, *60*(1), 208–221. https://doi.org/10.1016/j.datak.2006.01.013

Bivand, R. S., Pebesma, E., & Gómez-Rubio, V. (2013). *Applied Spatial Data Analysis with R*. Springer. https://doi.org/10.1007/978-1-4614-7618-4

Boonprong, S., Punturasan, N., Varnakovida, P., & Prechathamwong, W. (2024). Towards Sustainable Urban Mobility: Voronoi-Based Spatial Analysis of EV Charging Stations in Bangkok. *Sustainability*, *16*(11), 4729. https://doi.org/10.3390/su16114729

Byers, S., & Raftery, A. E. (1998). Nearest-Neighbor Clutter Removal for Estimating Features in Spatial Point Processes. *Journal of the American Statistical Association*, *93*(442), 577–584. https://doi.org/10.1080/01621459.1998.10473711

Campello, R. J. G. B., Moulavi, D., & Sander, J. (2013). Density-Based Clustering Based on Hierarchical Density Estimates. In J. Pei, V. S. Tseng, L. Cao, H. Motoda, & G. Xu (Eds.), *Advances in Knowledge Discovery and Data Mining* (pp. 160–172). Springer. https://doi.org/10.1007/978-3-642-37456-2_14

Chen, Y. (2023). Spatial autocorrelation equation based on Moran's index. *Scientific Reports*, *13*(1), 19296. https://doi.org/10.1038/s41598-023-45947-x

Dahim, M., Alqadhi, S., & Mallick, J. (2023). Enhancing landslide management with hyper-tuned machine learning and deep learning models: Predicting susceptibility and analyzing sensitivity and uncertainty. *Frontiers in Ecology and Evolution*, *11*, 1108924. https://doi.org/10.3389/fevo.2023.1108924

Dal Seno, N., Evangelista, D., Piccolomini, E., & Berti, M. (2024). Comparative analysis of conventional and machine learning techniques for rainfall threshold evaluation under complex geological conditions. *Landslides*, *21*(12), 2893–2911. https://doi.org/10.1007/s10346-024-02336-3

Density Estimation for Statistics and Data Analysis | Bernard. W. Silv. (n.d.). Retrieved March 23, 2025, from https://www.taylorfrancis.com/books/mono/10.1201/9781315140919/density-estimation-statistics-data-analysis-bernard-silverman

Ester, M., Kriegel, H.-P., Sander, J., & Xu, X. (1996a). A density-based algorithm for discovering clusters in large spatial databases with noise. *Proceedings of the Second International Conference on Knowledge Discovery and Data Mining, KDD'96*, 226–231.

Ester, M., Kriegel, H.-P., Sander, J., & Xu, X. (1996b). A density-based algorithm for discovering clusters in large spatial databases with noise. *Proceedings of the Second International Conference on Knowledge Discovery and Data Mining, KDD'96*, 226–231.

Gers, F. A., Schmidhuber, J., & Cummins, F. (2000). Learning to Forget: Continual Prediction with LSTM. *Neural Computation*, *12*(10), 2451–2471. https://doi.org/10.1162/089976600300015015

Getis, A., & Ord, J. K. (1992a). The Analysis of Spatial Association by Use of Distance Statistics. *Geographical Analysis*, *24*(3), 189–206. https://doi.org/10.1111/j.1538-4632.1992.tb00261.x

Getis, A., & Ord, J. K. (1992b). The Analysis of Spatial Association by Use of Distance Statistics. *Geographical Analysis*, *24*(3), 189–206. https://doi.org/10.1111/j.1538-4632.1992.tb00261.x

Ghasemian, B., Shahabi, H., Shirzadi, A., Al-Ansari, N., Jaafari, A., Kress, V. R., Geertsema, M., Renoud, S., & Ahmad, A. (2022). A Robust Deep-Learning Model for Landslide Susceptibility Mapping: A Case Study of Kurdistan Province, Iran. *Sensors*, *22*(4), 1573. https://doi.org/10.3390/s22041573

Graves, A., Mohamed, A., & Hinton, G. (2013). Speech recognition with deep recurrent neural networks. *2013 IEEE International Conference on Acoustics, Speech and Signal Processing*, 6645–6649. https://doi.org/10.1109/ICASSP.2013.6638947

Griffith, D. A. (2021). Interpreting Moran Eigenvector Maps with the Getis-Ord G_i * Statistic. *The Professional Geographer*, *73*(3), 447–463. https://doi.org/10.1080/00330124.2021.1878908

Guzzetti, F., Mondini, A. C., Cardinali, M., Fiorucci, F., Santangelo, M., & Chang, K.-T. (2012a). Landslide inventory maps: New tools for an old problem. *Earth-Science Reviews*, *112*(1–2), 42–66. https://doi.org/10.1016/j.earscirev.2012.02.001

Guzzetti, F., Mondini, A. C., Cardinali, M., Fiorucci, F., Santangelo, M., & Chang, K.-T. (2012b). Landslide inventory maps: New tools for an old problem. *Earth-Science Reviews*, *112*(1), 42–66. https://doi.org/10.1016/j.earscirev.2012.02.001

Hafsa, B., Chowdhury, Md. S., & Rahman, Md. N. (2022). Landslide susceptibility mapping of Rangamati District of Bangladesh using statistical and machine intelligence model. *Arabian Journal of Geosciences*, *15*(15), 1367. https://doi.org/10.1007/s12517-022-10607-3

Haining, R. (2003). *Spatial Data Analysis: Theory and Practice*. Cambridge University Press. https://doi.org/10.1017/CBO9780511754944

Han, J., Guo, X., Jiao, R., Nan, Y., Yang, H., Ni, X., Zhao, D., Wang, S., Ma, X., Yan, C., Ma, C., & Zhao, J. (2023). An Automatic Method for Delimiting Deformation Area in InSAR Based on HNSW-DBSCAN Clustering Algorithm. *Remote Sensing*, *15*(17), 4287. https://doi.org/10.3390/rs15174287

Hawkins, D. M. (1980). Outliers from the linear model. In D. M. Hawkins (Ed.), *Identification of Outliers* (pp. 85–103). Springer Netherlands. https://doi.org/10.1007/978-94-015-3994-4_7

He, K., Zhang, X., Ren, S., & Sun, J. (2015). Delving Deep into Rectifiers: Surpassing Human-Level Performance on ImageNet Classification. *2015 IEEE International Conference on Computer Vision (ICCV)*, 1026–1034. https://doi.org/10.1109/ICCV.2015.123

Hochreiter, S., & Schmidhuber, J. (1997). Long Short-Term Memory. *Neural Computation*, *9*(8), 1735–1780. https://doi.org/10.1162/neco.1997.9.8.1735

Humayain, K., & Biplob, C. (2021). *Landslide susceptibility mapping in the municipality of southeastern Bangladesh: The case of Rangamati district*. *14*.

Hussain, M. A., Chen, Z., Zhou, Y., Meena, S. R., Ali, N., & Shah, S. U. (2025). Landslide susceptibility mapping using artificial intelligence models: A case study in the Himalayas. *Landslides*. https://doi.org/10.1007/s10346-025-02466-2

Indra Prakash, Dam Duc Nguyen, Nguyen Thanh Tuan, Tran Van Phong, & Le Van Hiep. (2024). Landslide Susceptibility Zoning: Integrating Multiple Intelligent Models with SHAP Analysis. *Journal of Science and Transport Technology*, 23–41. https://doi.org/10.58845/jstt.utt.2024.en.4.1.23-41

Isnan, S., Bin Abdullah, A. F., Shariff, A. R., Ishak, I., Syed Ismail, S. N., & Appanan, M. R. (2025). Moran's *I* and Geary's *C*: Investigation of the effects of spatial weight matrices for assessing the distribution of infectious diseases. *Geospatial Health*, *20*(1). https://doi.org/10.4081/gh.2025.1277

Kingma, D. P., & Ba, J. (2017). *Adam: A Method for Stochastic Optimization* (arXiv:1412.6980). arXiv. https://doi.org/10.48550/arXiv.1412.6980

LeCun, Y., Bengio, Y., & Hinton, G. (2015). Deep learning. *Nature*, *521*(7553), 436–444. https://doi.org/10.1038/nature14539

Lu, J., Ren, C., Yue, W., Zhou, Y., Xue, X., Liu, Y., & Ding, C. (2023). Investigation of Landslide Susceptibility Decision Mechanisms in Different Ensemble-Based Machine Learning Models with Various Types of Factor Data. *Sustainability*, *15*(18), 13563. https://doi.org/10.3390/su151813563

Malamud, B. D., Turcotte, D. L., Guzzetti, F., & Reichenbach, P. (2004). Landslide inventories and their statistical properties. *Earth Surface Processes and Landforms*, *29*(6), 687–711. https://doi.org/10.1002/esp.1064

Memisoglu Baykal, T. (2025a). Performance assessment of GIS-based spatial clustering methods in forest fire data. *Natural Hazards*, *121*(7), 8445–8477. https://doi.org/10.1007/s11069-025-07135-0

Memisoglu Baykal, T. (2025b). Performance assessment of GIS-based spatial clustering methods in forest fire data. *Natural Hazards*, *121*(7), 8445–8477. https://doi.org/10.1007/s11069-025-07135-0

Miao, Z., Chen, Y., Zeng, X., & Li, J. (2016). Integrating Spatial and Attribute Characteristics of Extended Voronoi Diagrams in Spatial Patterning Research: A Case Study of Wuhan City in China. *ISPRS International Journal of Geo-Information*, *5*(7), 120. https://doi.org/10.3390/ijgi5070120

Mind'je, R., Li, L., Nsengiyumva, J. B., Mupenzi, C., Nyesheja, E. M., Kayumba, P. M., Gasirabo, A., & Hakorimana, E. (2020). Landslide susceptibility and influencing factors analysis in Rwanda. *Environment, Development and Sustainability*, *22*(8), 7985–8012. https://doi.org/10.1007/s10668-019-00557-4

Núñez, J. R., Anderton, C. R., & Renslow, R. S. (2018). Optimizing colormaps with consideration for color vision deficiency to enable accurate interpretation of scientific data | PLOS One. *PLOS ONE*, *13*(7), e0199239. https://doi.org/10.1371/journal.pone.0199239

Okabe, A., Boots, B., Sugihara, K., Chiu, S. N., & Kendall, D. G. (Eds.). (2000). *Spatial Tessellations*. John Wiley & Sons, Inc. https://doi.org/10.1002/9780470317013

Ord, J. K., & Getis, A. (1995). Local Spatial Autocorrelation Statistics: Distributional Issues and an Application. *Geographical Analysis*, *27*(4), 286–306. https://doi.org/10.1111/j.1538-4632.1995.tb00912.x

Parzen, E. (1962). On Estimation of a Probability Density Function and Mode. *The Annals of Mathematical Statistics*, *33*(3), 1065–1076. https://doi.org/10.1214/aoms/1177704472

Rabby, Y. W., Li, Y., Abedin, J., & Sabrina, S. (2022). Impact of Land Use/Land Cover Change on Landslide Susceptibility in Rangamati Municipality of Rangamati District, Bangladesh. *ISPRS International Journal of Geo-Information*, *11*(2), 89. https://doi.org/10.3390/ijgi11020089

Rahman, M. A., & Konagai, K. (2017). Substantiation of debris flow velocity from super-elevation: A numerical approach. *Landslides*, *14*(2), 633–647. https://doi.org/10.1007/s10346-016-0725-3

Rahman, Md. A., & Konagai, K. (2018). A hands-on approach to estimate debris flow velocity for rational mitigation of debris hazard. *Canadian Geotechnical Journal*, *55*(7), 941–955. https://doi.org/10.1139/cgj-2017-0211

Reichstein, M., Camps-Valls, G., Stevens, B., Jung, M., Denzler, J., Carvalhais, N., & Prabhat. (2019). Deep learning and process understanding for data-driven Earth system science. *Nature*, *566*(7743), 195–204. https://doi.org/10.1038/s41586-019-0912-1

Sameen, M. I., Pradhan, B., & Lee, S. (2020). Application of convolutional neural networks featuring Bayesian optimization for landslide susceptibility assessment. *CATENA*, *186*, 104249. https://doi.org/10.1016/j.catena.2019.104249

Schubert, E., Sander, J., Ester, M., Kriegel, H. P., & Xu, X. (2017). DBSCAN Revisited, Revisited: Why and How You Should (Still) Use DBSCAN. *ACM Trans. Database Syst.*, *42*(3), 19:1-19:21. https://doi.org/10.1145/3068335

Song, Y., Song, Y., Wang, C., Wu, L., Wu, W., Li, Y., Li, S., & Chen, A. (2024). Landslide susceptibility assessment through multi-model stacking and meta-learning in Poyang County, China. *Geomatics, Natural Hazards and Risk*, *15*(1), 2354499. https://doi.org/10.1080/19475705.2024.2354499

Srivastava, N., Hinton, G., Krizhevsky, A., Sutskever, I., & Salakhutdinov, R. (2014). Dropout: A simple way to prevent neural networks from overfitting. *J. Mach. Learn. Res.*, *15*(1), 1929–1958.

Virtanen, P., Gommers, R., Oliphant, T. E., Haberland, M., Reddy, T., Cournapeau, D., Burovski, E., Peterson, P., Weckesser, W., Bright, J., van der Walt, S. J., Brett, M., Wilson, J., Millman, K. J., Mayorov, N., Nelson, A. R. J., Jones, E., Kern, R., Larson, E., … van Mulbregt, P. (2020). SciPy 1.0: Fundamental algorithms for scientific computing in Python. *Nature Methods*, *17*(3), 261–272. https://doi.org/10.1038/s41592-019-0686-2

Xiao, X., Zou, Y., Huang, J., Luo, X., Yang, L., Li, M., Yang, P., Ji, X., & Li, Y. (2024). An interpretable model for landslide susceptibility assessment based on Optuna hyperparameter optimization and Random Forest. *Geomatics, Natural Hazards and Risk*, *15*(1), 2347421. https://doi.org/10.1080/19475705.2024.2347421

Yang, X., Tang, L., Zhang, X., & Li, Q. (2018). A Data Cleaning Method for Big Trace Data Using Movement Consistency. *Sensors*, *18*(3), 824. https://doi.org/10.3390/s18030824

Yang, X., Vannier, J., Yang, J., Wang, D., & Zhang, X. (2021). Priapulid worms from the Cambrian of China shed light on reproduction in early animals. *Geoscience Frontiers*, *12*(6), 101234. https://doi.org/10.1016/j.gsf.2021.101234

Yu, M., Chen, L., Fan, X., Ma, P., Zhao, S., Wu, Z., Yang, F., Xu, L., Shan, M., Xie, X., Zeng, H., & Zhang, Z. (2025). Validating and enhancing data-driven landslide susceptibility prediction by model explanation and MT-InSAR techniques. *International Journal of Digital Earth*, *18*(1), 2509857. https://doi.org/10.1080/17538947.2025.2509857